ELSEVIER

www.elsevier.nl/locate/jorganchem

Journal of Organometallic Chemistry 605 (2000) 117–126

Journal of Organometallic Chemistry

Rhodium complexes with hydrotris(3-*p*-anisylpyrazol-1-yl)borate ligand Tp^{pAn}. Intramolecular C–H bond activation and dehydro-chlorination processes☆

M.D. Santa María* [a,1], R.M. Claramunt [a], J.A. Campo [b], M. Cano* [b,2], R. Criado [b], J.V. Heras [b], P. Ovejero [b], E. Pinilla [b], M.R. Torres [b]

[a] *Departamento de Química Orgánica y Biología, Facultad de Ciencias, Universidad Nacional de Educación a Distancia, Senda del Rey 9, E-28040 Madrid, Spain*

[b] *Departamento de Química Inorgánica I, Laboratorio de Difracción de Rayos-X, Facultad de Ciencias Químicas, Universidad Complutense, E-28040 Madrid, Spain*

Received 6 April 2000; received in revised form 5 May 2000

Abstract

Solution studies by ^{1}H- and ^{13}C-NMR, and IR spectroscopy of rhodium(I) complexes [Rh(η^4-nbd)(Tp^{pAn})] (**1**), [Rh(η^4-cod)(Tp^{pAn})] (**2**) and [Rh(CO)$_2$(Tp^{pAn})] (**3**) (nbd = 2,5-norbornadiene; cod = cycloocta-1,5-diene) have been performed. In all cases square planar complexes containing the Tp^{pAn} ligand in a bidentate η^2-bonded form were observed. Compounds **2** and **3** exist as mixtures of two isomers with the third uncoordinated pyrazolyl ring occupying an equatorial position (form **A**) or an axial position (form **B**), but in complex **1** only form **B** is present. X-ray crystallography proved that complexes **1** and **3** are also tetracoordinated in solid state: **1** (monoclinic, space group $P2_1/c$) and **3** (monoclinic, space group $P2_1/c$), whose structures correspond to two different **B** forms, their difference lying in the disposition of the axial pyrazolyl group. Photochemical irradiation of [Rh(CO)$_2$(Tp^{pAn})] (**3**) in a variety of solvents afforded the aryl hydride [Rh(H)(CO){HB($C_3H_2N_2C_6H_3OCH_3$)($C_3H_2N_2C_6H_4OCH_3$)$_2$}] (**4**) by intramolecular cyclometallation involving an *ortho* C–H bond of one *p*-anisyl substituent. Functionalization of the hydride **4** by chlorinated solvents resulted in the chloro complex [Rh(Cl)(CO){HB($C_3H_2N_2C_6H_3OCH_3$)($C_3H_2N_2C_6H_4OCH_3$)$_2$}] (**5**), which maintains the intramolecular *ortho* C–metal bond. Evolution of the hydride **4** to the chloro complex **5** in $CDCl_3$ occurs through a hydrodechlorination process as deduced by monitoring the NMR spectra. Analysis of 2D NMR data (^{1}H–^{1}H COSY, ^{1}H–^{13}C HMQC and ^{1}H–^{13}C HMBC) allowed the full identification of **4** and **5**.

Keywords: Trispyrazolylborates; Rhodium complexes; NMR spectroscopy; Crystal structures; Photochemistry; C–H bond activation

1. Introduction

The photochemical activation of alkanes, alkenes, and arenes, starting from organometallic precursors has been continuous over the years since the pioneer works of Janowickz and Bergman [2], using [Ir(η^5-C_5Me_5)H_2(PMe_3)], and Hoyano et al. [3], using [Ir(CO)$_2$(η^5-C_5Me_5)]. Mechanisms of C–H bond activation reactions in Rh and Ir complexes of types [Rh(CO)$_2$(Tp^{Me2})] and [Ir(η^4-cod)(Tp^{Me2})] (cod = cycloocta-1,5-diene) have been recently proposed [4–6]. Dechelation and rechelation of Tp ligands are proposed as determinant steps on the C–H bond activation [7].

We report here the structural studies on three new Rh complexes, [Rh(η^4-nbd)(Tp^{pAn})] (**1**) (nbd = 2,5-norbornadiene), [Rh(η^4-cod)(Tp^{pAn})] (**2**) and [Rh(CO)$_2$(Tp^{pAn})] (**3**) in solution and in the solid state, in order to establish the coordination type η^2- or η^3-Tp^{pAn} of the existing species. It has now been extensively proved that the denticity of the Tp-type ligands accounts for the reactivity of Rh and Ir complexes and therefore their catalytic applications [4,5].

☆ Tp^{pAn} is the abbreviation used by Trofimenko for the hydrotris(3-*p*-anisylpyrazol-1-yl)borate [1].

[1] *Corresponding author.

[2] *Corresponding author.

0022-328X/00/$ - see front matter
PII: S0022-328X(00)00283-7

The photochemical reactivity, at room temperature (r.t.) and pressure, of $[Rh(CO)_2(Tp^{pAn})]$ (**3**) in alkanes and benzene is also discussed. In all cases, intramolecular attack of ligand *p*-anisyl substituent C–H bonds with formation of an aryl hydride *ortho*-metalated $[Rh(H)(CO)\{HB(C_3H_2N_2C_6H_3OCH_3)(C_3H_2N_2C_6H_4OCH_3)_2\}]$ (**4**) is observed. Functionalization of the hydride complex **4** to the chloride derivative *ortho*-metalated $[Rh(Cl)(CO)\{HB(C_3H_2N_2C_6H_3OCH_3)(C_3H_2N_2C_6H_4OCH_3)_2\}]$ (**5**) was produced by reaction with CCl_4.

In addition, the evolution of **4** to **5** in $CDCl_3$ was monitored by ^{1}H-NMR experiments. This process occurs with a C–Cl bond cleavage through an intermediate complex in which the solvent is implicated [8–12]. Scheme 1 shows the molecular structure of complexes **1**–**5**.

2. Experimental

2.1. Materials and instrumentation

Literature methods were used to prepare 3(5)-*p*-anisylpyrazole and the hydrotris(3-*p*-anisylpyrazol-1-yl)borate as potassium or thallium salt, KTp^{pAn} or $TlTp^{pAn}$ [13]. The organometallic starting materials $Rh_2Cl_2(nbd)_2$ and $Rh_2Cl_2(cod)_2$ were obtained as described in references [14,15]. All the reactions were performed at r.t. and an inert atmosphere was not necessary. Commercial solvents were dried prior to use.

Elemental analyses for carbon, hydrogen and nitrogen were carried out by the Microanalytical Service of the Complutense University of Madrid. IR spectra were recorded either as KBr discs or in solution in NaCl cells on an FT-IR Nicolet Magna 550 spectrometer. FAB mass spectra (*m*-NBA matrix) were obtained on a VG AutoSpec spectrometer.

NMR spectra were obtained on a Bruker DRX-400 spectrometer at 27°C. ^{1}H and ^{13}C chemical shifts (ppm) are downfield from TMS using $CDCl_3$ ($\delta_H = 7.26$ ppm, $\delta_C = 77.0$ ppm) as the internal standard. The following NMR experiments with pulse field gradients, (^{1}H–^{1}H) COSY and (^{1}H–^{13}C) HMQC and HMBC were used [16].

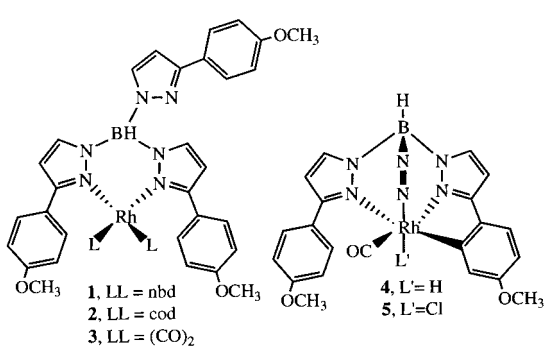

Scheme 1.

2.2. Synthesis of $[Rh(\eta^4\text{-nbd})(Tp^{pAn})]$ (**1**) and $[Rh(\eta^4\text{-cod})(Tp^{pAn})]$ (**2**)

To a solution of $Rh_2Cl_2(diolefin)_2$ (diolefin = nbd, cod) (0.2 mmol) in dichloromethane (15 ml), 0.4 mmol of KTp^{pAn} or $TlTp^{pAn}$ were added. The clear yellow–orange solution was stirred for 2 h and then the solvent was removed at reduced pressure. The solid residue was solved in 5 ml of dichloromethane and the solution filtered through Celite. The solution was evaporated off and then the yellow–orange solid treated with diethyl ether, the solvent evaporated off again and the solid dried under vacuum.

2.2.1. $[Rh(\eta^4\text{-nbd})(Tp^{pAn})]$ (**1**)

Yield: 90%. Anal. Found: C, 61.23; H, 5.06; N, 11.27. Calc. for $C_{37}H_{36}BN_6O_3Rh$: C, 61.18; H, 5.0; N, 11.57%.

2.2.2. $[Rh(\eta^4\text{-cod})(Tp^{pAn})]$ (**2**)

Yield: 95%. Anal. Found: C, 61.05; H, 5.35; N, 11.49. Calc. for $C_{38}H_{40}BN_6O_3Rh$: C, 61.47; H 5, 43; N, 11.32%.

2.3. Synthesis of $[Rh(Tp^{pAn})(CO)_2]$ (**3**)

Carbon monoxide was bubbled through a solution of $[Rh(Tp^{pAn})(diolefin)]$ (**1**) or (**2**) (0.1 mmol) in dichloromethane (15 ml) at r.t. and atmospheric pressure for 45 min. The yellow solid obtained after removal of the solvent was treated with diethyl ether and evaporated again to dryness. The yellow solid was dried under vacuum. Yield: 85%. Anal. Found: C, 56.19; H, 4.42; N, 11.67. Calc. for $C_{32}H_{28}BN_6O_5Rh$: C, 55.68; H, 4.09; N, 12.17%.

^{1}H-NMR (400 MHz): Form **A**: δ 6.37 (1H, d, ^3J(HH) 2.5 Hz, H-4 ring 1), 6.56 (1H, d, ^3J(HH) 2.3 Hz, H-4 ring 2), 6.57 (1H, d, ^3J(HH) 2.3 Hz, H-4 ring 3), 7.15 (1H, d, ^3J(HH) 2.5 Hz, H-5 ring 1), 8.05 (1H, d, ^3J(HH) 2.3 Hz, H-5 ring 2), 8.51 (1H, d, ^3J(HH) 2.3 Hz, H-5 ring 3), 7.95 (2H, d, ^3J(HH) 8.8 Hz, $2H_{ortho}$ ring 1), 7.85 (2H, d, ^3J(HH) 8.8 Hz, $2H_{ortho}$ ring 2), 7.79 (2H, d, ^3J(HH) 8.8 Hz, $2H_{ortho}$ ring 3), 6.97 (2H, d, ^3J(HH) 8.8 Hz, $2H_{meta}$ ring 1), 7.11 (2H, d, ^3J(HH) 8.8 Hz, $2H_{meta}$ ring 2), 7.06 (2H, d, ^3J(HH) 8.8 Hz, $2H_{meta}$ ring 3), 3.85 (3H, s, OCH_3 ring 1), 3.93 (3H, s, OCH_3 ring 2) and 3.90 (3H, s, OCH_3 ring 3); Form **B**: δ 6.44 (3H, br s, 3H-4), 7.70 (3H, br s, 3H-5), 7.82 (6H, br s, $6H_{ortho}$), 7.02 (6H, br s, $6H_{meta}$) and 3.88 (9H, s, $3OCH_3$).

^{13}C-NMR (400 MHz): Form **A**: δ 156.5 (C-3 ring 1), 157.2 (C-3 ring 2), 156.8 (C-3 ring 3), 105.5 (C-4 ring 1), 105.9 (C-4 ring 2), 105.6 (C-4 ring 3), 137.5 (C-5 ring 1),

Table 1
Crystal and refinement data for [Rh(η⁴-nbd)(Tp^pAn)] (**1**) and [Rh(CO)₂(Tp^pAn)] (**3**)

Compound	**1**	**3**
Formula	$C_{37}H_{36}BN_6O_3Rh$	$C_{32}H_{28}BN_6O_5Rh$
Molecular weight	726.44	690.32
Crystal system	Monoclinic	Monoclinic
Space group	$P2_1/c$	$P2_1/c$
a (Å)	8.201(4)	9.014(2)
b (Å)	15.399(8)	16.970(4)
c (Å)	28.781(6)	20.674(6)
β (°)	95.36(1)	98.77(2)
V (Å^3)	3619(3)	3126(1)
Z	4	4
D_{calc} (g cm^{-3})	1.333	1.467
Temperature (K)	295	295
μ(Mo–K$_\alpha$) (mm^{-1})	0.515	0.597
Crystal size (mm)	0.2×0.15×0.15	0.2×0.1×0.1
Scan technique	$\omega/2\theta$	$\omega/2\theta$
θ (°)	$1<\theta<25$	$1<\theta<25$
Index ranges (hkl) (°)	(−9, 0, 0) to (9, 18, 34)	(−10, 0, 0) to (10, 20, 24)
No. reflections collected	5746	5547
No. independent reflections	5636	5389
R_{int}	0.0965	0.1009
Data/restraints/parameters	5636/0/433	5389/0/406
$R=[\Sigma\|F_o\|-\|F_c\|/\Sigma\|F_o\|]$	0.062 (2229 reflections observed)	0.0506 (1755 reflections observed)
wR [a]	0.1562	0.1182

[a] $wR=[\Sigma w(|F_o|^2-|F_c|^2)^2\Sigma w|F_o|^2)^2]^{1/2}$.

140.1 (C-5 ring 2), 142.5 (C-5 ring 3), 125.8 (C_{ipso} ring 1), 125.1 (C_{ipso} ring 2), 125.5 (C_{ipso} ring 3), 130.6 ($2C_{ortho}$ ring 1), 130.6 ($2C_{ortho}$ ring 2),), 130.9 ($2C_{ortho}$ ring 3), 113.5 ($2C_{meta}$ ring 1), 114.0 ($2C_{meta}$ ring 2), 113.8 ($2C_{meta}$ ring 3), 160.0 (C_{para} ring 1), 160.8 (C_{para} ring 2), 160.7 (C_{para} ring 3), 55.2, 55.38 and 55.42 ($3OCH_3$), 184.2 (1C, d, J(RhC) 68.3 Hz, CO) and 182.4 (1C, d, J(RhC) 68.2 Hz, CO); Form **B**: δ 155.0 (3C-3, br s), 104.4 (3C-4, br s), 137.0 (3C-5, br s), 126.4 ($3C_{ipso}$, br s), 130.2 ($6C_{ortho}$, br s), 113.8 ($6C_{meta}$, br s), 160.0 ($3C_{para}$, br s), 55.32 ($3OCH_3$, br s) and 183.3 (2C, d, J(RhC) 68.7 Hz, CO).

2.4. Synthesis of [Rh(H)(CO){HB(C$_3$H$_2$N$_2$C$_6$H$_3$OCH$_3$)-(C$_3$H$_2$N$_2$C$_6$H$_4$OCH$_3$)$_2$}] (**4**)

A suspension of [Rh(Tp^pAn)(CO)$_2$] (**3**) (50 mg, 0.072 mmol) in n-pentane (80 ml) was irradiated under dinitrogen atmosphere with a 450 W Hanovia medium pressure mercury lamp for 1 h. The mixture was filtered over Celite giving rise a colorless solution. Then the solvent was evaporated to dryness, yielding the hydridorhodium(III) complex **4** as a white solid which was dried under vacuum. This compound was kept under dinitrogen in a refrigerator. Yield: 30%. Anal. Found: C, 55.91; H, 4.33; N, 12.0. Calc. for $C_{31}H_{28}BN_6O_4Rh$: C, 56.22; H, 4.26; N, 12.69%.

2.5. Synthesis of xz c[Rh(Cl)(CO){HB(C$_3$H$_2$N$_2$C$_6$-H$_3$OCH$_3$)(C$_3$H$_2$N$_2$C$_6$H$_4$OCH$_3$)$_2$}] (**5**)

To the colorless solution of **4** in n-pentane obtained as explained previously (after filtration over Celite), CCl_4 (1 ml) was added under dinitrogen atmosphere, stirred for 1 h and then filtered. The solution was kept in the freezer overnight. The formed pale yellow solid **5** was separated off and dried under vacuum. Yield: 60%. Anal. Found: C, 53.02; H, 4.25; N, 11.65. Calc. for $C_{31}H_{27}BClN_6O_4Rh$: C, 53.44; H, 3.91; N, 12.06%. FAB mass spectra: 697 $[M+H]^+$, 668 $[M-CO]^+$, 661 $[M-Cl]^+$, 633 $[RhTp^{pAn}]^+$.

2.6. Synthesis of [Rh(CO)(Tp^{pAn})(μ-OH)]$_2$ (**6**)

A colorless solution of **4** in n-pentane was kept in the freezer for 1 day. [Rh(CO)(Tp^pAn)(μ-OH)]$_2$ (**6**) was obtained as a white solid after filtration and drying. Yield: 60%. Anal. Found: C, 54.7; H, 4.12; N, 11.5. Calc. for $C_{62}H_{56}B_2N_{12}O_{10}Rh_2$: C, 54.88; H, 4.17; N, 12.39%. FAB mass spectra: 1355 $[M-H]^+$, 1311 $[M-CO-OH]^+$, 661 $[RhCOTp^{pAn}]^+$, 633 $[RhTp^{pAn}]^+$.

2.7. Structure determination

Yellow prismatic single crystals were obtained for [Rh(η⁴-nbd)(Tp^pAn)] (**1**) and [Rh(CO)$_2$(Tp^pAn)] (**3**) from dichloromethane. The data were collected on an Enraf–Nonius CAD-4 diffractometer and unit cell constants were refined from least-squares fitting of the θ values of 25 reflections with 2θ 8–24° for **1** and 2θ 6–28° for **3**. A summary of the fundamental crystal data is given in Table 1.

Three check reflections were monitored after every 97 reflections for both compounds. No appreciable drop in the intensities of standard reflections was observed. The coordinates of the Rh atom were determined from a 3D Patterson synthesis and the positions of all other non-hydrogen atoms obtained by Fourier methods. They were refined by full-matrix least-squares on F^2 SHELXL-97 [17]. All non-hydrogen atoms have been refined anisotropically.

Hydrogen atoms were calculated and refined as a riding on carbon bonded atom with a common isotropic displacement parameters, except the hydrogen atom of the boron which has been found as the first peak in a difference Fourier syntheses, including fixed positions. The largest residual peak in the final difference map was 0.55 and 0.40 e Å^{-3} for **1** and **3**, respectively, in the vicinity of the Rh atom.

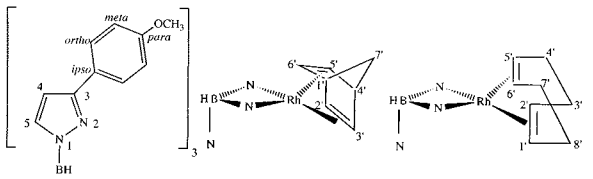

Fig. 1. Atomic numbering used in the NMR assignments.

3. Results and discussion

3.1. Synthesis and solution structural studies of [Rh(η⁴-nbd)(Tp^pAn)] (1), [Rh(η⁴-cod)(Tp^pAn)] (2) and [Rh(CO)₂(Tp^pAn)] (3)

The potassium or thallium salt of the tris(3-*p*-anisylpyrazol-1-yl)borate, KTp^{pAn} or $TlTp^{pAn}$, reacted with the binuclear rhodium complexes $[Rh_2Cl_2(\eta^4\text{-nbd})_2]$ and $[Rh_2Cl_2(\eta^4\text{-cod})_2]$ in dry dichloromethane to afford $[Rh(\eta^4\text{-nbd})(Tp^{pAn})]$ (**1**) and $[Rh(\eta^4\text{-cod})(Tp^{pAn})]$ (**2**). $[Rh(CO)_2(Tp^{pAn})]$ (**3**) was obtained by bubbling a stream of carbon monoxide throughout a dichloromethane solution of **1** or **2**.

^{1}H- and ^{13}C-NMR chemical shift data of the $[Rh(\eta^4\text{-nbd})(Tp^{pAn})]$ (**1**), $[Rh(\eta^4\text{-cod})(Tp^{pAn})]$ (**2**) and $[Rh(CO)_2(Tp^{pAn})]$ (**3**) (see Fig. 1 for NMR atomic numbering), indicate that the coordination mode of the hydrotris(3-*p*-anisylpyrazol-1-yl)borate ligands is similar to the one found in rhodium complexes of hydrotris(3-phenylpyrazol-1-yl)borate ligands [18], where the three isomers **A**–**C** were encountered (Scheme 2).

The ^{1}H-NMR data in $CDCl_3$ solution of $[Rh(\eta^4\text{-nbd})(Tp^{pAn})]$ (**1**) show all three 3-*p*-anisylpyrazolyl groups equivalent, δ 6.43 (3H, br s, 3H-4), 7.73 (3H, br s, 3H-5), 3.08 (2H, br s, H-1′, 4′), 2.91 (4H, br s, H-2′, 3′, 5′, 6′), 0.70 (2H, br s, CH_2-7′), 7.93 (6H, d, ^3J(HH) 8.8 Hz, $6H_{ortho}$), 7.03 (6H, d, ^3J(HH) 8.8 Hz, $6H_{meta}$) and 3.89 (9H, s, $3OCH_3$). This magnetic equivalence can be explained as due to: (i) form **B** in which a fast exchange between coordinated and free pyrazolyl forms takes place; (ii) form **C**; or even (iii) a fast equilibrium between four- and five-coordinated complexes of types **B** and **C**. These processes may be difficult to differentiate, besides the trigonal bipyramid–square pyramid interconversion in five coordinated species [18].

However, after examining the ^{13}C-NMR data obtained in $CDCl_3$ solution for compound **1**: δ 153.8 (3C-3, br s), 103.8 (3C-4, br s), 136.4 (3C-5, br s), 49.8 (C-1′, 4′), 57.2 (C-2′, 3′, 5′, 6′, br s), 62.0 (C-7′), δp-anisyl carbons: 126.8 ($3C_{ipso}$, br s), 129.0 ($6C_{ortho}$, br s), 113.5 ($6C_{meta}$, br s), 159.5 ($3C_{para}$, br s) and 55.4 ($3OCH_3$, br s), where the nbd chemical shifts follow the standard sequence δC-7′ > δC-2′, 3′, 5′, 6′ > δC-1′, 4′, we are able to conclude that this complex exists in a tetracoordinated form **B**. In pentacoordinated forms, δC-2′, 3′, 5′, 6′ appear at about 40 ppm [18].

The situation is more complicated for compound $[Rh(\eta^4\text{-cod})(Tp^{pAn})]$ (**2**), which in $CDCl_3$ solution is a mixture of two tetracoordinated forms **A** and **B** (52**A**/48**B**). In Table 2 are presented the ^{1}H- and ^{13}C-NMR chemical shifts for the complex **2** in $CDCl_3$, with complete assignments to forms **A** and **B** based on symmetry considerations and 2D experiments.

Here again the ^{13}C chemical shifts for the olefinic carbons of the ancillary ligand cod in solution were crucial to confirm that only tetracoordinated forms are present in the $[Rh(\eta^4\text{-cod})(Tp^{pAn})]$ spectra. The δC-1′, 2′, 5′, 6′ appeared at 78.6 and 83.1 ppm for isomer **A** and 81.3 ppm for isomer **B** in $CDCl_3$ solution, in agreement with a chemical shift of around 80 ppm considered to be normal for the olefinic carbon resonance in four-coordinate Rh–cod complexes.

^{1}H- and ^{13}C-NMR spectra in $CDCl_3$ of a sample of $[Rh(CO)_2(Tp^{pAn})]$ (**3**) obtained by 'slow crystallization' showed the equivalence of the 3-*p*-anisylpyrazolyl rings, which indicate that only the **B** isomer is present. Nevertheless, signals for the **A** and **B** forms appeared in a ratio of 45/55 in the spectra of a 'fast crystallization' sample in dichloromethane (see Section 3.2).

IR analysis of compounds **1**–**3** revealed that the band corresponding to the ν(BH) absorption appears

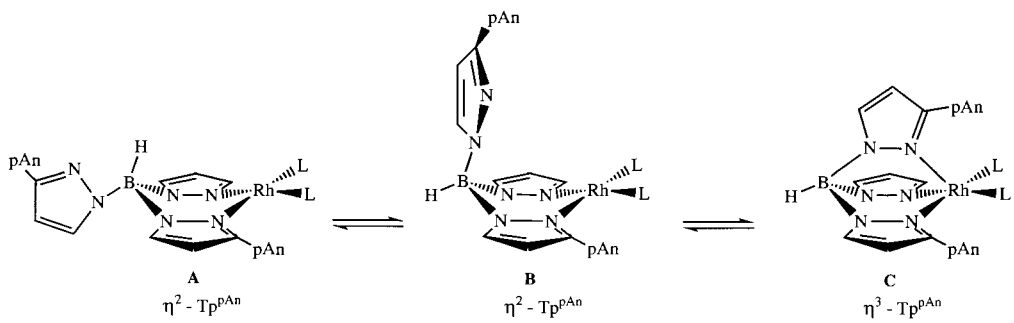

Scheme 2. Isomeric forms for complexes $[Rh(L_2)(Tp^{pAn})]$.

Table 2
^{1}H- and ^{13}C-NMR data (chemical shifts, δ (in ppm) and coupling constants, J (in Hz)) of [Rh(η^4-cod)(Tp^{pAn})] (**2**)

Form **A** ($CDCl_3$)

cod	H-2′, 5′	C-2′, 5′	H-3′, 4′*exo*	H-3′, 4′*endo*	C-3′, 4′			
	3.35	78.6 J(Rh) = 12.4	2.03	1.51	30.0			
	H-1′, 6′	C-1′, 6′	H-7′, 8′*exo*	H-7′, 8′*endo*	C-7′, 8′			
	3.89	83.1 J(Rh) = 12.4	2.44	1.68	30.2			
Pyrazole	H-4	C-4	H-5	C-5	C-3			
	6.70 (1H) ^{3}J(H-5) = 2.1	101.7 (1C)	8.08 (1H)	138.8 (1C)	153.7 (1C)			
	6.22 (2H) ^{3}J(H-5) = 2.1	104.4 (2C)	7.42 (2H)	135.4 (2C)	153.3 (2C)			
p-An	H_{ortho}	C_{ortho}	H_{meta}	C_{meta}	C_{para}	C_{ipso}	H_{OMe}	C_{OMe}
	7.91 (2H) $^{3}J(H_{meta})$ = 8.7	129.7 (2C)	6.95 (2H)	113.8 (2C)	158.9 (1C)	127.5 (1C)	3.84 (3H)	55.2 (1C)
	8.04 (4H) $^{3}J(H_{meta})$ = 8.5	129.7 (4C)	7.11 (4H)	113.5 (4C)	159.8 (2C)	126.1 (2C)	3.94 (6H)	55.4 (2C)

Form **B** ($CDCl_3$)

cod	H-2′, 5′, 1′, 6′	C-2′, 5′, 1′, 6′	H-3′, 4′, 7′, 8′*exo*	H-3′, 4′, 7′, 8′*endo*	C-3′, 4′, 7′, 8′			
	3.42	81.3	1.68	1.18	29.3			
Pyrazole	H-4	C-4	H-5	C-5	C-3			
	6.46 (3H)	104.4 (3C)	7.84 (3H)	137.4 (3C)	154.0 (3C)			
p-An	H_{ortho}	C_{ortho}	H_{meta}	C_{meta}	C_{para}	C_{ipso}	H_{OMe}	C_{OMe}
	7.98 (6H) $^{3}J(H_{meta})$ = 7.7	128.9 (6C)	7.04 (6H)	113.6 (6C)	159.4 (3C)	127.0 (3C)	3.89 (9H)	55.3 (3C)

at lower frequency than 2470 cm^{-1} both in dichloromethane solution and in the solid state (compound **1**: KBr, 2419 cm^{-1}, CH_2Cl_2, 2427 cm^{-1}; compound **2**: KBr, 2404 cm^{-1}, CH_2Cl_2, 2409 cm^{-1}; compound **3**: KBr, 2440 cm^{-1}, CH_2Cl_2, 2445 cm^{-1}). These values are indicative of a η^2-Tp^{pAn} coordination in agreement with previous studies on RhTp complexes [19].

*3.2. X-ray crystal structures of [Rh(η^4-nbd)(Tp^{pAn})] (**1**) and [Rh(CO)$_2$(Tp^{pAn})] (**3**)*

The X-ray crystalline structures of [Rh(η^4-nbd)(Tp^{pAn})] (**1**) and [Rh(CO)$_2$(Tp^{pAn})] (**3**) revealed neutral species. A selection of bond lengths and angles, with their standard deviations is given in Table 3.

As can be observed in the PLUTO views of both molecules shown in Figs. 2 and 3, the rhodium atom in a square-planar coordination mode is bonded to two pyrazolyl rings of the η^2-bidentate hydrotris(3-*p*-anisylpyrazol-1-yl)borate ligand Tp^{pAn}, and the centroids of the nbd (C1122, C4455) double bonds in complex **1** or the carbon atoms of the carbonyl groups in complex **3**. This disposition gives a boat conformation metallocycle Rh(NN)$_2$B with the third pyrazole group in an axial position in both cases. In [Rh(η^4-nbd)(Tp^{pAn})] (**1**) the nbd is disposed in an orthogonal orientation with respect to the coordination plane. The least-square plane C1C2C4C5 forms a dihedral angle of 85.3(4)° with the least-square coordination plane (Table 4) [20].

However, there is a very important difference in the spatial orientation of the uncoordinated pyrazole, in **1** it occupies a parallel position with respect to the plane defined by Rh–C1–C5 (Rh–N32 = 3.67(1) and Rh–C35 = 3.59(1) Å, see Table 3). In [Rh(CO)$_2$(Tp^{pAn})] (**3**), the non-coordinating pyrazole is situated perpen-

dicular to the coordination plane with the N32 atom towards the rhodium atom (Rh–N32 2.57(1) Å). Moreover, the Rh atom is included in the best least-square

Table 3
Selected bond distances (Å) and angles (°) for [Rh(η⁴-nbd)(Tp^{pAn})] (**1**) and [Rh(CO)$_2$(Tp^{pAn})] (**3**) with estimated S.D. values in parentheses

Compound	**1**		**3**
Rh–C1			1.82(1)
Rh–C2			1.84(1)
Rh–N12	2.111(9)		2.108(7)
Rh–N22	2.087(9)		2.111(8)
Rh–C1122	2.00(1)		
Rh–C4455	1.99(1)		
C1–C2	1.40(2)		
C4–C5	1.40(2)		
B–N11	1.54(2)		1.52(1)
B–N21	1.55(2)		1.56(1)
B–N31	1.54(2)		1.56(2)
B–H	1.021		1.202
Rh···B	3.23(1)		3.30(1)
Rh···N32	3.67(1)		2.57(1)
Rh···C35	3.59(1)		4.46(1)
N22–Rh–N12	84.7(4)	N22–Rh–N12	86.0(3)
N22–Rh–C1122	100.9(4)	N22–Rh–C1	94.7(4)
N22–Rh–C4455	172.0(4)	N22–Rh–C2	176.1(4)
N12–Rh–C1122	170.6(4)	N12–Rh–C1	169.7(4)
N12–Rh–C4455	102.9(4)	N12–Rh–C2	93.9(4)
C1122–Rh–C4455 [a]	71.2(4)	C1–Rh–C2	84.6(4)

[a] C1122 and C4455 are the midpoints of the olefinic bonds C1, C2 and C4, C5

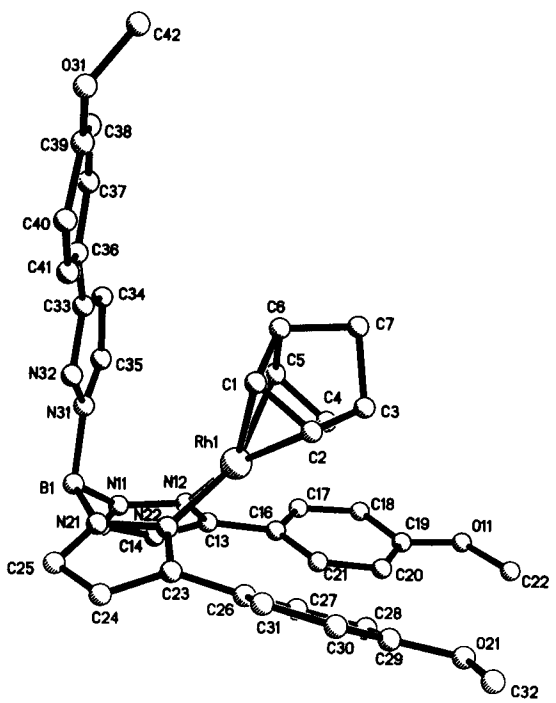

Fig. 2. PLUTO view of [Rh(η⁴-nbd)(Tp^{pAn})] (**1**). The hydrogen atoms have been omitted.

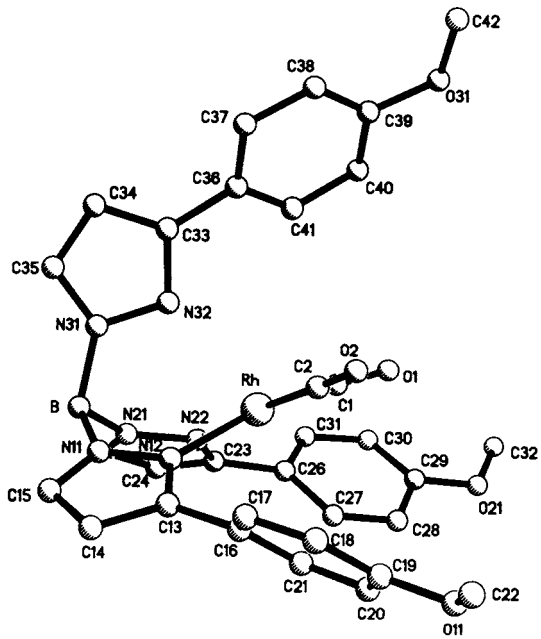

Fig. 3. PLUTO view of [Rh(CO)$_2$(TppAn)] (**3**). The hydrogen atoms have been omitted.

Table 4
Selected angles (°) between the least-squares sets defined by the specified atoms for [Rh(η⁴-nbd)(Tp^{pAn})] (**1**) and [Rh(CO)$_2$(Tp^{pAn})] (**3**)

	Planes	
	1	**3**
1-	N12,N22,C1122,C4455	N12,N22, C1,C2
2-	N11,N12,C13,C14,C15	N11,N12,C13,C14,C15
3-	N21,N22,C23,C24,C25	N21,N22,C23,C24,C25
4-	N31,N32,C33,C34,C35	N31,N32,C33,C34,C35
5-	C16,C17,C18,C19,C20,C21	C16,C17,C18,C19,C20,C21
6-	C26,C27,C28,C29,C30,C31	C26,C27,C28,C29,C30,C31
7-	C36,C37,C38,C39,C40,C41	C36,C37,C38,C39,C40,C41
1–2	46.5(4)	37.8(4)
1–3	49.7(4)	33.7(3)
1–4	39.5(4)	80.6(3)
2–3	55.1(4)	53.7(4)
2–4	77.9(4)	66.3(4)
3–4	85.3(4)	61.0(4)
2–5	48.3(4)	54.4(4)
3–6	41.2(4)	55.9(3)
4–7	9.2(4)	38.2(4)

coordination plane in the nbd derivative **1**, but is outside this plane at a distance of 0.1248 (9) Å towards the N32 atom in the dicarbonyl derivative **3**.

The axial disposition is the most frequent one encountered in related compounds [18,21–27], as opposed to the equatorial one [18,28]. Only in a few cases, which correspond to dicarbonyl complexes, do we find the nitrogen atom towards the rhodium one [21,22] as we describe here for the [Rh(CO)$_2$(Tp^{pAn})] (**3**) derivative. All the η²-bidentate complexes show shorter bond dis-

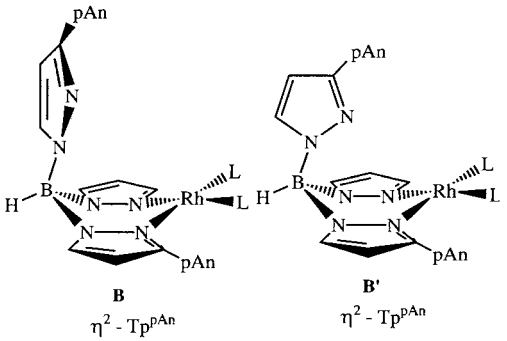

Fig. 4. η^2-Tp^{pAn} forms **B** and **B′** for $[Rh(CO)_2(Tp^{pAn})]$ (**3**).

tances Rh–N than the η^3-coordinated, as already pointed out by Rheingold et al. [26].

In addition the torsion angles between the planes of the pyrazole rings and their 3-*p*-anisyl substituents are also different in both complexes. The greatest difference appears in the uncoordinated axial 3-*p*-anisylpyrazole, the values for such angles being of 9.2(4) and 38.2(4)° for **1** and **3**, respectively (Table 4). In the similar complex $[Rh(\eta^4\text{-nbd})(Tp^{Ph})]$, the uncoordinated axial pyrazole and its 3-phenyl group are twisted by 21.1(1)° [18].

The crystal packings of the two compounds present a different propeller-like disposition of the methoxy groups of the *p*-anisyl substituent. In **1** all of them turn in the same direction, while in the carbonyl derivative **3**, two methoxy groups are oriented to one side and the third one to the opposite one. These characteristics must be regarded as essentially solid-state packing effects.

Lastly, it must be pointed out that the crystals of **3** analyzed by X-ray difraction were obtained from a dichloromethane solution when the crystallization process was performed at low temperature (4–5°C) over several days (2–3) ('slow crystallization'). Such crystals were identified as a new η^2-Tp^{pAn}, from here named **B′** (Fig. 4) intermediate form between **B** and **C**, where the free pyrazolyl ring is rotated towards the Rh atom (Rh–N = 2.57 Å). By contrast the rapid evaporation of the solvent gives rise to a solid compound identified as a mixture of **A** and **B** ('fast crystallization').

An IR spectrum in the solid state of a sample of **3** obtained by fast crystallization presents four bands at 2086, 2024 cm^{-1} of the **B** isomer and 2074, 2000 cm^{-1} of the **A** isomer. However, crystals formed by slow crystallization, form **B′**, show two strong bands at lower frequencies, 2056 and 1987 cm^{-1}. This IR bands shift implicates a higher back-bonding to the CO ligands as a consequence of a greater electronic density on the Rh atom. The η^2-**B′** form exists only in solid state.

3.3. Intramolecular C–H bond activation in $[Rh(CO)_2(Tp^{pAn})]$ (3)

The **B** or **B′** forms, but not the **A** isomer, of the Rh $[Rh(CO)_2(Tp^{pAn})]$ (**3**) intramolecularly activate the *ortho* C–H bond of one *p*-anisylpyrazolyl group, by irradiation of their solutions in several solvents (*n*-pentane, cyclohexane and benzene) at r.t., producing the hydride complex $[Rh(H)(CO)\{HB(C_3H_2N_2C_6H_3OCH_3)(C_3H_2N_2C_6H_4OCH_3)_2\}]$ (**4**). It is interesting to note that the activation process is cleaner in pentane than in the other solvents. The IR spectrum of **4** in KBr shows a strong ν(CO) and a weak ν(Rh–H) bands at 2056 and 2084 cm^{-1}, respectively.

NMR spectroscopic data for complex **4** are consistent with an intramolecular aryl C–H bond activation reaction from $[Rh(CO)_2(Tp^{pAn})]$ (**3**). A freshly prepared solution of **4** in $CDCl_3$ at 300 K shows three sets of ligand resonances, in a ratio 1:1:1, due to the 3-*p*-anisylpyrazolyl groups and a doublet at −14.37 ppm (J(Rh–H) 22.8 Hz) of the hydride in the ^{1}H-NMR spectrum. The proton and carbon signals have been assigned without ambiguity using 2D NMR methods (see Scheme 3): (^{1}H–^{1}H) COSY to identify the hydrogen atoms and (^{1}H–^{13}C) HMQC and HMBC to determine the corresponding ^{13}C chemical shift values (in parentheses).

Intramolecular C–H bond activation using Tp^{Ph} systems have previously been studied [29], so some parallel experiments with Tp^{Ph} and Tp^{pAn} systems were compared and the expected enhancement on activation rate observed for the latter in agreement with the electrophilic nature of the process.

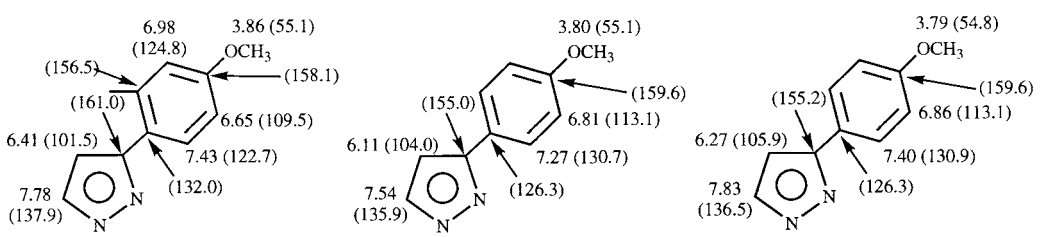

Scheme 3. ^{1}H- and ^{13}C-NMR (in parentheses) chemical shifts values of the 3-*p*-anisylpyrazolyl rings in $[Rh(H)(CO)\{HB(C_3H_2N_2C_6H_3OCH_3)(C_3H_2N_2C_6H_4OCH_3)_2\}]$ (**4**).

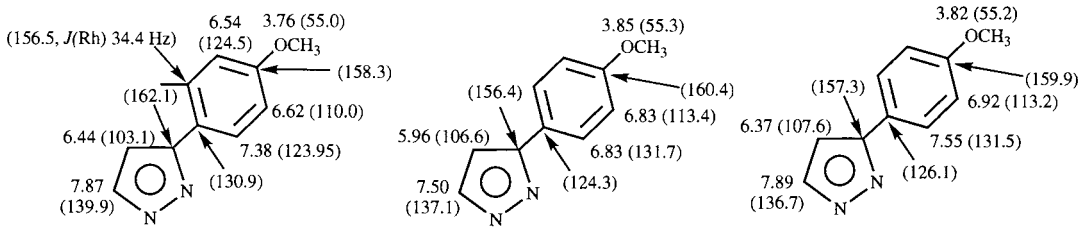

Scheme 4. ^{1}H- and ^{13}C-NMR (in parentheses) chemical shifts values of the 3-*p*-anisylpyrazolyl rings in [Rh(Cl)(CO){HB($C_3H_2N_2C_6H_3OCH_3$)($C_3H_2N_2C_6H_4OCH_3)_2$}] (**5**).

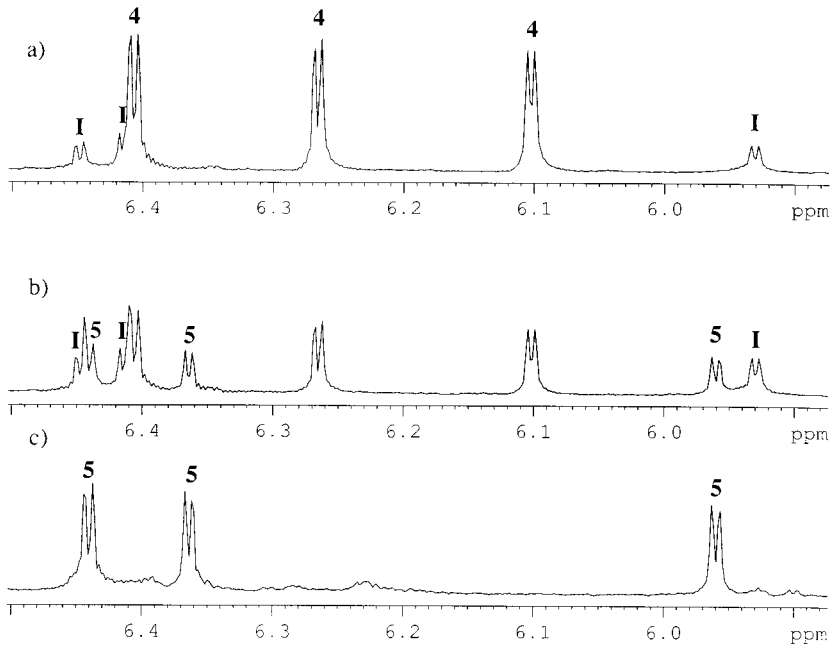

Fig. 5. ^{1}H-NMR spectra (H-4 protons zone) which show the evolution of the hydride [Rh(H)(CO){HB($C_3H_2N_2C_6H_3OCH_3$)($C_3H_2N_2C_6H_4OCH_3)_2$}] (**4**) in $CDCl_3$ solution at 300 K. (a) Freshly prepared, (b) after 25 min, and (c) after 21 h.

By addition of CCl_4 to a freshly solution of sample **4** in pentane, the related chloride derivative [Rh(Cl)(CO){HB($C_3H_2N_2C_6H_3OCH_3$)($C_3H_2N_2C_6H_4O$-$CH_3)_2$}] (**5**) was isolated. The IR and NMR spectroscopic data of **5** are consistent with a functionalization of the hydride to the chloride derivative in which the *ortho*-metalation is maintained. The ν(CO) band was moved to 2086 cm^{-1} with respect to that at 2056 cm^{-1} in **4**, in agreement with the substitution of H by Cl ligand. The assignments of the hydrogen and carbon atoms associated with each 3-*p*-anisylpyrazolyl subunit in complex **5** were obtained using 2D correlation experiments (Scheme 4).

Finally the evolution at 300 K of the hydride **4** towards complex **5** in $CDCl_3$ solution was monitored by ^{1}H-NMR spectroscopy. As shown in Fig. 5(a), in the freshly prepared solution besides the characteristic pattern of the hydride **4**, small signals at 5.93, 6.42 and 6.45 ppm of an intermediate appeared, for which we postulate structure **I** (see Scheme 5) that fulfil the electronic and structural requirements around the metallic center. The ^{1}H-NMR signal for the hydrido intermediate **I** is probably overlapped by the one corresponding to **4**. After 25 min, the spectrum presented also signals due to the chloride complex **5**: H-4 protons at 5.96, 6.37 and 6.44 ppm (Fig. 5(b)). It is interesting to note that from this moment a signal at 5.29 ppm (not shown in Fig. 5) corresponding to $CHDCl_2$ (J(HD) 1.1 Hz) was observed, whose intensity increases during the evolution as well as those of the chloride derivative **5** indicating an hydrodechlorination process of the solvent. After 21 h in $CDCl_3$ solution, only signals of **5** and $CHDCl_2$ remained (Fig. 5(c)).

A related process (Scheme 5) was observed in the evolution of the hydride complex **4** when water traces were present in the solvent, the final compound being $[Rh(CO)(Tp^{pAn})(\mu\text{-}OH)]_2$ (**6**), (ν(CO) = 2090 cm^{-1} (in KBr); ν(CO) = 2094 cm^{-1} and ν(OH) = 3507 cm^{-1} (in CCl_4 solution); $M^+ = 1355$).

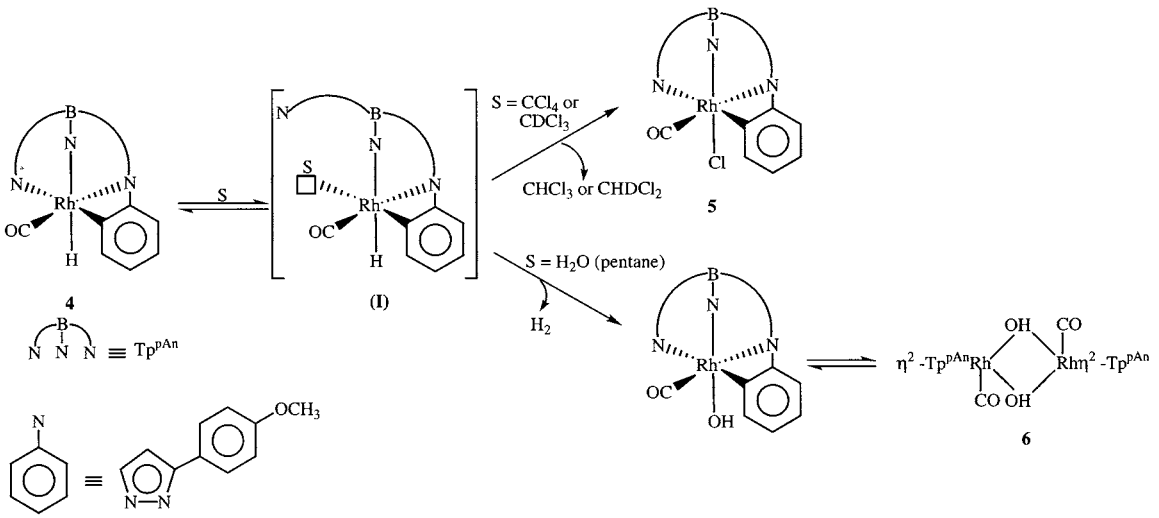

Scheme 5. Evolution of the aryl hydride [Rh(H)(CO){HB($C_3H_2N_2C_6H_3OCH_3$)($C_3H_2N_2C_6H_4OCH_3$)$_2$}] (**4**) in different solvents.

4. Concluding remarks

The coordination mode of hydrotris(3-*p*-anisylpyrazol-1-yl)borate ligand, Tp^{pAn}, in Rh(I) complexes of type [Rh(LL)(Tp^{pAn})] (LL = nbd, cod, $(CO)_2$) **1**–**3** has been studied. In thje solid state, X-ray crystallography and IR spectroscopy reveal the η^2-denticity of the chelating ligand in [Rh(η^4-nbd)(Tp^{pAn})] (**1**), [Rh(η^4-cod)(Tp^{pAn})] (**2**) and [$Rh(CO)_2(Tp^{pAn})$] (**3**), in agreement with what we encountered in the same type of complexes for Tp^{Ph} ligand [18].

In solution, a dynamic equilibrium between two isomeric forms: **A**, a tetracoordinated square-planar complex with two coordinated pyrazolyl groups and the uncoordinated one in equatorial position, and **B**, a tetracoordinated square-planar with two coordinated pyrazoles and the third one in axial position, is evidenced.

The photochemical behavior of [$Rh(CO)_2(Tp^{pAn})$] (**3**) in alkanes and benzene proved that an intramolecular attack of ligand *p*-anisyl substituent C–H bond with formation of an aryl hydride *ortho*-metalated [Rh(H)(CO){HB($C_3H_2N_2C_6H_3OCH_3$)($C_3H_2N_2C_6H_4OCH_3$)$_2$}] (**4**) occurred. Functionalization of **4** by chlorinated solvents gives rise to [Rh(Cl)(CO){HB($C_3H_2N_2C_6H_3OCH_3$)($C_3H_2N_2C_6H_4OCH_3$)$_2$}] (**5**). Evolution of **4** to **5** through intermediates in which the solvents intervene complexing the metal was also confirmed.

5. Supplementary material

Crystallographic data (excluding structure factors) for the structures **1** and **3** reported in this paper have been deposited with the Cambridge Crystallographic Data Centre as supplementary publication nos. CCDC-127372 and -127373. Copies of the data can be obtained free of charge on application to CCDC, 12 Union Road, Cambridge CB2 1EZ, UK (fax: +44-1223-336033; e-mail: deposit@ccdc.cam.ac.uk; www: http://www.ccdc.cam.ac.uk).

Acknowledgements

We are indebted to DGES/MEC of Spain for financial support (PB96-0001-C03-01 and PB95-0370) and Comunidad de Madrid (07N /0001 /1999).

References

[1] (a) S. Trofimenko, Chem. Rev. 93 (1993) 943. (b) S. Trofimenko, Scorpionates: The Coordination Chemistry of Polypyrazolylborate Ligands, Imperial College Press, London, 1999.
[2] (a) A. Janowickz, R.G. Bergman, J. Am. Chem. Soc. 104 (1982) 352. (b) A. Janowickz, R.G. Bergman, J. Am. Chem. Soc. 105 (1983) 3929.
[3] (a) J.K. Hoyano, W.A.G. Graham, J. Am. Chem. Soc. 104 (1982) 3723. (b) J.K. Hoyano, A.D. McMaster, W.A.G. Graham, J. Am. Chem. Soc. 105 (1983) 7190.
[4] S.E. Bromberg, H. Yang, M.C. Asplund, T. Lian, B.K. McNamara, K.T. Kotz, J.S. Yeston, M. Wilkens, H. Frei, R. Bergman, C.B. Harris, Science 28 (1997) 260 and Refs. cited therein.
[5] A. Ferrari, M. Merlin, S. Sostero, O. Traverso, H. Ruegger, L.M. Venanzi, Helv. Chim. Acta 81 (1998) 2127 and Refs. cited therein.
[6] A.A. Purwoko, A.J. Lees, Inorg. Chem. 35 (1996) 675.
[7] M. Roubi, Chem. Eng. News 75 (1997) 4.
[8] V.V. Grushin, H. Alper, Organometallics 10 (1991) 1620.
[9] D.T. Ferrughelli, I.T. Horvath, J. Chem. Soc. Chem. Commun. (1992) 806.
[10] M. Huser, M.-T. Youinou, J.A. Osborn, Angew. Chem. Int. Ed. Engl. 28 (1989) 1386.
[11] H. Nishiyama, M. Horihata, T. Hirai, S. Wakamatsu, K. Itoh, Organometallics 10 (1991) 2706.

[12] M.A. Ciriano, M.A. Tena, L.A. Oro, J. Chem. Soc. Dalton Trans. (1992) 2123.
[13] S. Trofimenko, J.C. Calabrese, J.K. Kochi, S. Wolowiec, F.B. Hulsbergen, J. Reedjik, Inorg. Chem. 31 (1992) 3943.
[14] E.W. Abel, M.A. Bennett, G. Wilkinson, J. Chem. Soc. A (1959) 3178.
[15] J. Chatt, L.M. Venanzi, J. Chem. Soc. (1957) 4735.
[16] S. Braun, H.-O. Kalinowski, S. Berger, 100 and More Basic NMR Experiments, VCH, New York, 1996.
[17] G.M. Sheldrick, SHELXL-97, Program for Crystal Structure Refinement, University of Göttingen, Germany, 1997.
[18] (a) U.E. Bucher, A. Currao, R. Nesper, H. Rüegger, L.M. Venanzi, E. Younger, Inorg. Chem. 34 (1995) 66. (b) D. Sanz, M.D. Santa María, R.M. Claramunt, M. Cano, J.V. Heras, J.A. Campo, F.A. Ruíz, E. Pinilla, A. Monge, J. Organomet. Chem. 526 (1996) 341.
[19] M. Akita, K. Ohta, Y. Takahashi, S. Hikichi, Y. Moro-oka, Organometallics 16 (1997) 4121.
[20] M. Nardelli, PARST-97, University of Parma, Italy, 1997.
[21] A.L. Rheingold, R.L. Ostrader, B.S. Haggerty, S. Trofimenko, Inorg. Chem. 33 (1994) 3666.
[22] E. del Ministro, O. Reun, H. Rueger, L.M. Venanzi, U. Burckhardt, V. Gramlich, Inorg. Chim. Acta 240 (1995) 631.
[23] R.G. Ball, C.K. Gosh, J.K. Hoyano, A.D. McMaster, W.A.G. Graham, J. Chem. Soc. Chem. Commun. (1989) 341.
[24] V. Chauby, C.S. Le Berre, Ph. Kalch, J.C. Daran, G. Comenges, Inorg. Chem. 35 (1996) 6354.
[25] M. Akita, K. Ohta, Y. Takahashi, S. Hikichi, Y. Moro-oka, Organometallics 16 (1997) 4121.
[26] A.L. Rheingold, B.S. Haggerty, G.P.A. Yap, S. Trofimenko, Inorg. Chem. 36 (1997) 5097.
[27] W.D. Jones, E.T. Hessl, Inorg. Chem. 30 (1991) 778.
[28] M.C. Keyes, V.G. Young Jr., W.B. Tolman, Organometallics 15 (1996) 4133.
[29] R. Krentz, Ph.D. Thesis, Model Compounds in Carbon–Hydrogen Activation, University of Alberta, Canada, 1989.